

Nonlinear Finite Element Analysis of Anchored Blind-Bolted Joints to Concrete-Filled Steel Tubular Columns

Yihuan Wang^{a,b}, Zhan Wang^{a,b}, Jianrong Pan^{a,b,*}, and Peng Wang^a

^a*Department of Civil Engineering, South China University of Technology, Guangzhou, 510640, China*

^b*State Key Laboratory of Subtropical Building Science, South China University of Technology, Guangzhou, 510640, China*

Abstract

A nonlinear finite element analysis (FEA) on rectangular concrete-infilled tubular (CFT) column connections was conducted using the FEA software ABAQUS. In this analysis, loading path and stress distribution of the anchored blind-bolted (ABB) connections to CFT columns were clearly defined; influences of strength grade of bolts, thickness of endplates, vertical interval between bolts, diameter of bolts, and pretension on bolts on the studied connections were determined. The results of FEA indicate that the flush endplate connections of ABB CFT columns are typical semi-rigid connections. The established finite element (FE) model was verified by test results of six anchored blind-bolted flush endplate connections to CFT columns. The test results show that the model can accurately simulate mechanical performance of the ABB connections and is suitable for different forms of ABB connections to CFT columns.

Keywords: finite element analysis; anchored blind bolt; Hollo-Bolt; concrete-infilled steel tubular column connections; parameter analysis

(Submitted on November 13, 2018; Revised on December 8, 2018; Accepted on January 10, 2019)

© 2019 Totem Publisher, Inc. All rights reserved.

1. Introduction

CFT columns have been widely applied in practical projects due to their excellent structural performance, low cost, and convenient erection [1]. It is, however, difficult to connect steel tubes with H-shape steel beams because of closed cross section of the tubes. To solve this problem, a blind-bolted connection technology, in which bolts are installed from the beam side only without access within the column section, has been developed abroad in recent years.

One of the most commonly used blind bolts is the Hollo-Bolt (Figure 1(a)), which was invented by the Lindapter International Company of England. Scholars have conducted numerous studies on this type of blind bolt. Ellison and Tizani [2] conducted monotonic loading tests on four T-shaped endplate connections to CFT columns to study the mechanical performances of different blind-bolted connections. The Hollo-Bolt showed lower stiffness but better ductility than other types of blind bolts. According to EC3, the CFT column connections using Hollo-Bolts are classified into semi-rigid connection. Elghazouli et al. [3] used the Hollo-Bolt as blind bolts in 17 top and bottom angle connections between rectangular steel tubular columns and steel beams, and they conducted monotonic loading and reversed cyclic loading tests on them. Their tests showed that this type of connection demonstrates excellent rotation performance, which conforms to the design requirements. Furthermore, a simplified calculation model for the initial stiffness and moment capacity of the connections was established through the tests. Wang et al. [4-6] used the Hollo-Bolt to conduct monotonic loading tests on eight flush endplate connections to CFT columns and cyclic loading tests on four outrigger endplate connections to CFT columns. On the basis of the stiffness, strength, and hysteresis characteristics of the connections, they concluded that when the CFT connections connected by the Hollo-Bolt are subjected to flexure, the compression area can be supported by the infilled concrete; by contrast, the tensile area is always the weak part due to the low outward bending stiffness of the rectangular steel tubular walls, thereby limiting the performance of the connections. Tizani et al. [7] modified the Hollo-Bolt by extension of threaded rods and installation of a nut at the end for anchoring, similar to a headed stud, as shown in Figure 1(b). Pitrakos and Tizani [8] systematically studied the tensile performance of the modified Hollo-Bolt, analyzed the influences of different parameters on its tensile performance and indicated that the modified Hollo-Bolt can display the full

* Corresponding author.

E-mail address: ctjrpan@scut.edu.cn

tensile capacity of the threaded rod. Tizani and Wang et al. [9-10] used the modified Hollo-Bolt to conduct monotonic loading and cyclic loading tests on flush endplate connections to CFT columns. The tests showed that such connections have two failure modes, namely bolt shank rupture and bolt pull-out, and exhibit high ductility and energy dissipation performance. Tizani [11] conducted tensile tests on ten T-shaped connections to CFT columns and studied the tensile capacity of high-strength bolts, blind bolts, the Hollo-Bolt, and the modified Hollo-Bolt when the rectangular steel tubes are hollow or filled with concrete. It is indicated that the connections have higher tensile capacity with the presence of concrete and the modified Hollo-Bolt demonstrates better tensile performance.

However, given that the structure of ABB CFT column connections is complex, their structural forms and relevant variable parameters are numerous. It is uneconomical and infeasible to study every influencing factor through tests. As an alternative, FEA can be used to study the nonlinear performance of ABB connections. The established FE model can be further utilized in the comprehensive finite element nonlinear parameter analysis on the different forms and structures of such connections.

In this study, a FE model of the ABB connections to CFT columns was established using the FEA software ABAQUS. The modified Hollo-Bolt shown in Figure 1(b) was selected as the anchored blind bolts. The elastoplasticity, large deformation, and contact problems were considered in the simulation. The results of six ABB flush endplate connections to CFT columns were used to be consistent with the FE model. Finally, a reasonable FE model for such connections was established. The load transfer modes and stress distribution of the ABB connections to CFT columns were analyzed using the verified FE model. The influencing factors on the performance of such connections were also analyzed. Furthermore, the effects of strength grade of bolts, thickness of endplates, vertical interval between bolts, diameter of bolts, and pretension on bolts on the connections were analyzed. The analysis results provide a reference for the design of anchored blind-bolted connections to CFT columns.

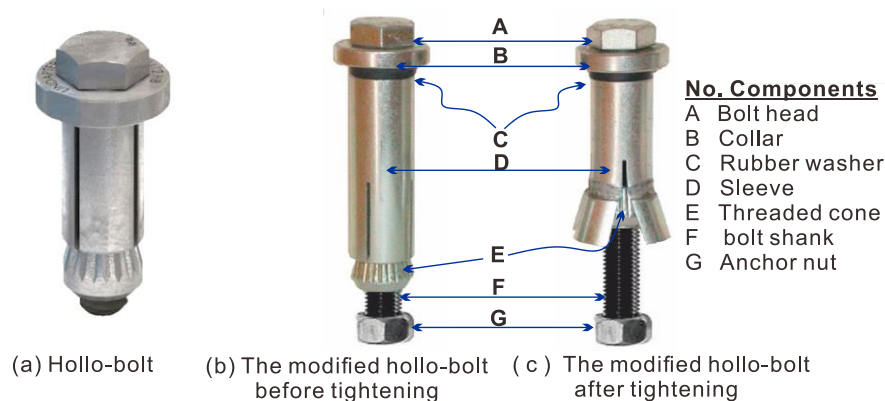


Figure 1. Schematic diagram of anchored Hollo-Bolt

2. Finite Element Modeling

In view of the material nonlinearity, geometric nonlinearity, and contact nonlinearity, the FEA software ABAQUS is adopted for the finite element analysis in this study, as the software has a strong nonlinearity function and allows for a convenient contact analysis.

2.1. Material Models

In consideration of the plastic hardening of the material and incremental theory of plasticity, ideal plastic material is added to guarantee certain hardening characteristics. The stress-strain relationship of the steel can be simplified as Figure 2, with the material constitutive curve presented by Bahaari and Sherbourne [12]. The Mises yield criterion is adopted to judge yield point of steel in the multiaxial stress state. When the equivalent stress of the steel exceeds the yield stress, the steel will undergo plastic deformation.

The plastic damage model is used for the concrete material model. The core concrete in the CFT is restricted by the steel tubes; thus, its properties are changed, that is, the plasticity of the concrete increases. The common uniaxial loading tests of concrete cannot reflect the change in plastic performance. Confinement of steel tubes to core concrete is considered by modified peak stress and descending line of the constitutive curve plateaus in the model. The uniaxial

constitutive model advised by Han et al. [13] is adopted for the core concrete as follows:

$$y = \begin{cases} 2x - x^2, & x \leq 1 \\ \frac{x}{\beta_0(x-1)^\eta + x}, & x > 1 \end{cases} \quad (1)$$

Where $x = \varepsilon/\varepsilon_0$, $y = \sigma/\sigma_0$, $\varepsilon_0 = \varepsilon_c + 800\varepsilon^{0.2} \times 10^{-6}$, and $\varepsilon_c = (1300 + 12.5f_c)$, where f_c is the compression strength of the concrete (N/mm²).

For rectangular steel tubes,

$$\eta = 1.6 + \frac{1.5}{x} \quad (2)$$

$$\beta_0 = \frac{f_c^{0.1}}{1.2\sqrt{1+\zeta}} \quad (3)$$

Where ζ is the confinement factor.

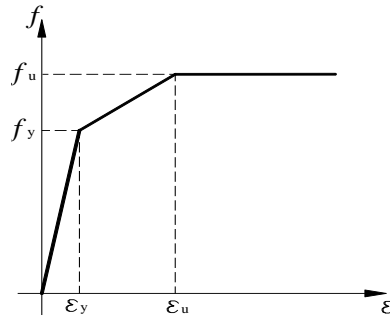


Figure 2. Trilinear model

2.2. Finite Element Modeling

The FE model is established using ABAQUS. All parts are modeled using the solid C3D8R, a linear displacement interpolation brick with reduced integration. The model is divided into six parts, namely endplate, h-shaped beam, steel tubular wall, bolt, sleeve, and concrete. In order to simplify the model, the bolt and nut are placed in same component, and the influence of welding is ignored. The h-shaped beam and endplate are tied, and the other components are connected using the tangential penalty function and normal hard contact. The shapes and mesh division diagrams of the components are shown in Figure 3. Numerous elements are generated by the refinement of the concrete mesh; thus, half of the symmetric model is adopted to improve the calculation efficiency. The model assembly is shown in Figure 4. As the test loading is controlled by displacement, the finite element load is applied by establishing reference points coupled with the loading surface and by applying a certain displacement value.

3. Test Overview

Six ABB flush endplate connections were designed to connect h-shaped s to square CFT columns. The details of the specimens are shown in Table 1. A schematic diagram of connection specimens is shown in Figure 5. The blind bolts adopted the modified grade 8.8 M16 Hollo-Bolt with an anchored nut. The anchorage depth of the nut was 90mm. The CFT column had a cross section of 250×250mm. The variable parameters were the column wall thickness, endplate thickness steel beam section, and anchorage method. Here, the column wall thickness could be changed by the plug welding of two 7 mm-C-shaped channels around the column wall in panel zone. The Hollo-Bolt used in specimen ST-5 was not anchored with a nut at the end of the threaded rod. Q235 steel was used for the weak beam flange and web in specimen ST-5, and the other steel material was Q345 steel. The compression strength and elastic modulus of concrete were 39.92MPa and 3.27×104MPa, respectively. The nominal yield stress of the grade 8.8 M16 Hollo-Bolt was 640MPa, and the ultimate stress was 800MPa. The elastic modulus of the Hollo-Bolt was 206GPa.

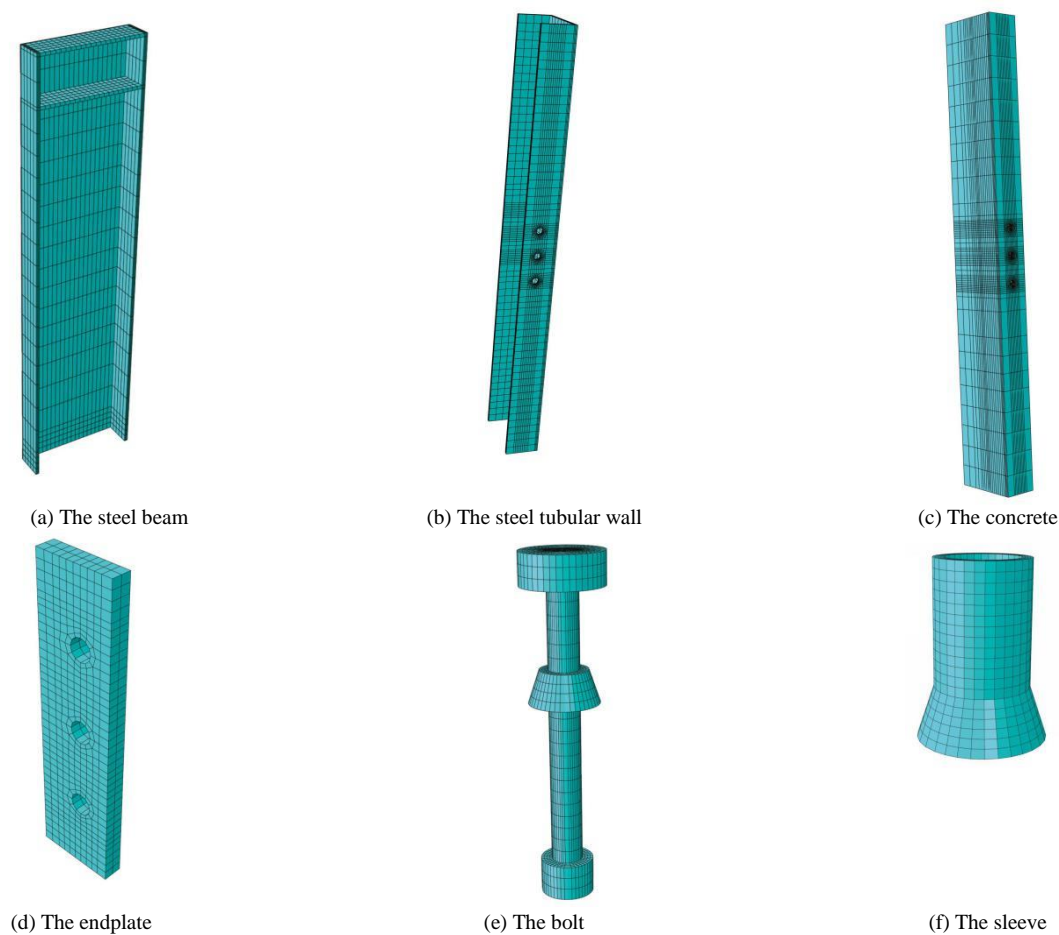


Figure 3. Mesh division diagrams of the different components

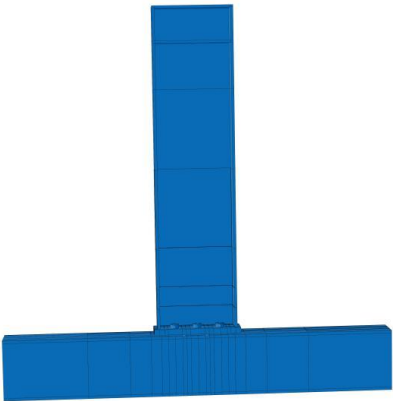
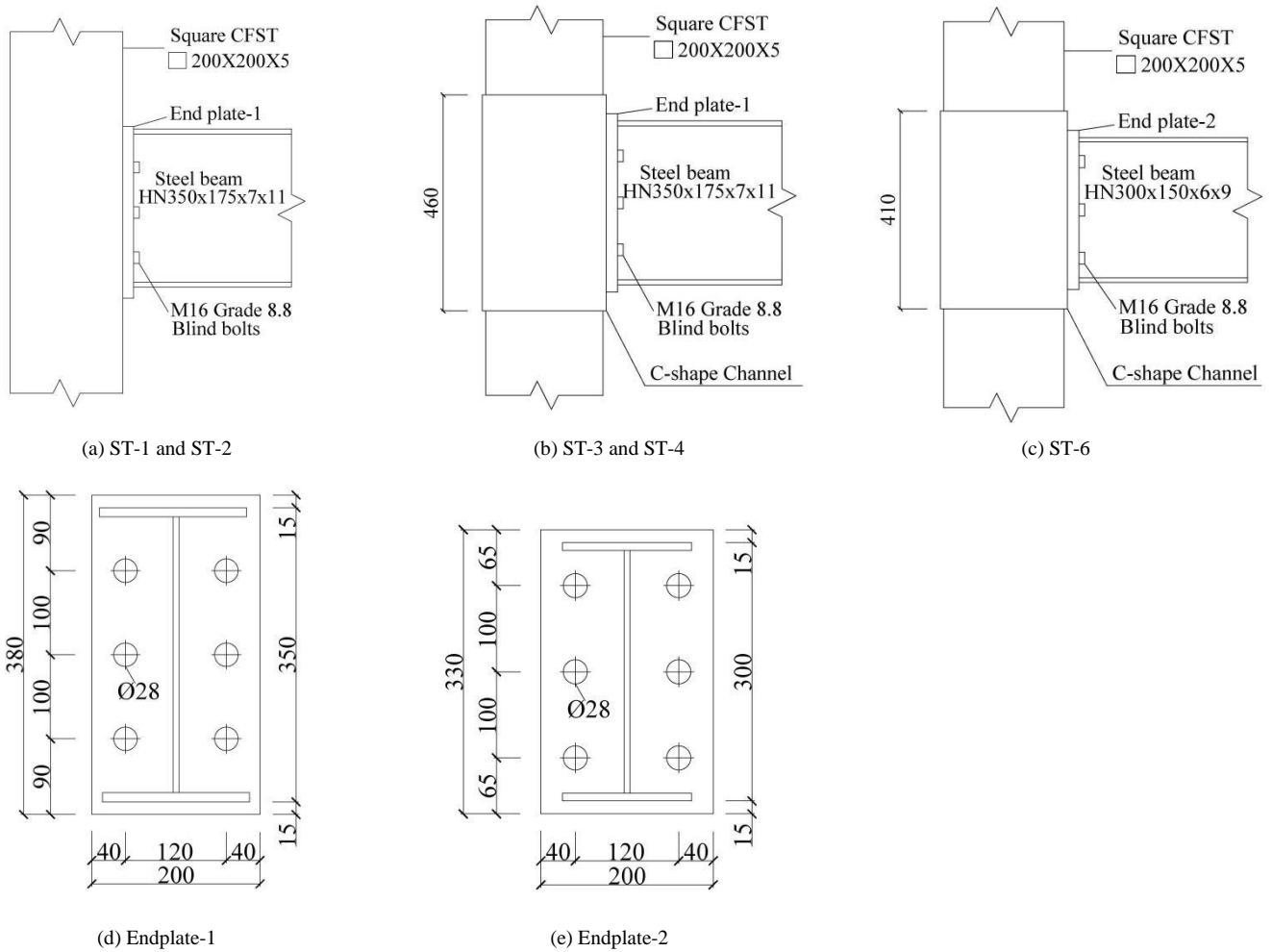


Figure 4. Model assembly diagram

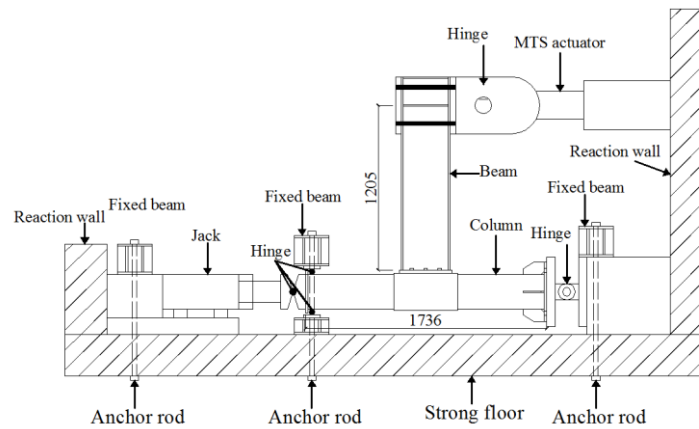
Table 1. Details of test specimens (Unit: mm)

Specimen	Column section	Column length	Beam section	Beam length	Endplate thickness	Local reinforcement	Anchorage method
ST-1	250×5	1736	HN350×175×7×11	1400	12	None	Nut
ST-2	250×5	1736	HN350×175×7×11	1400	24	None	Nut
ST-3	250×5	1736	HN350×175×7×11	1400	12	With	Nut
ST-4	250×5	1736	HN350×175×7×11	1400	24	With	Nut
ST-5	250×5	1736	HN350×175×7×11	1400	24	With	No
ST-6	250×5	1736	HN300×150×6×9	1400	24	With	Nut



Note: Specimens ST-4 and ST-5 have the same dimension, except ST-4 with nut and ST-5 without nut.
Figure 5. Schematic diagram of joint specimens

The test setup is shown in Figure 6. The beam was connected to the MTS hydraulic actuator through the loading plate. Both ends of CFTs were hinged with the reaction wall. Using a hydraulic jack, A 980kN axial load was applied to the column. The ratio of axial load was 0.3 for the CFT columns. The loading was controlled by progressive displacement as suggested by SAC-97 1997 [14] (Figure 7). The test terminated when the connections could not carry loads or the loading device limit was reached.



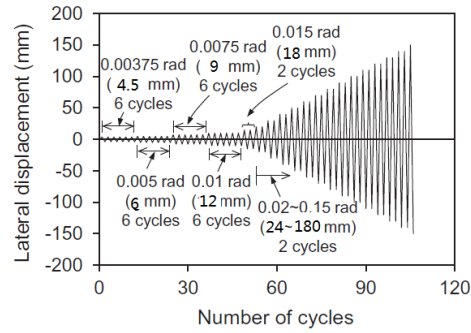
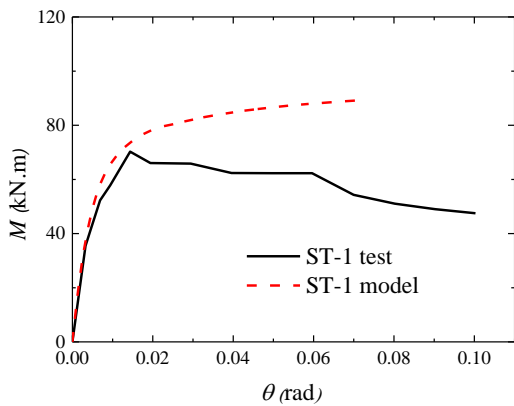


Figure 7. Loading protocol

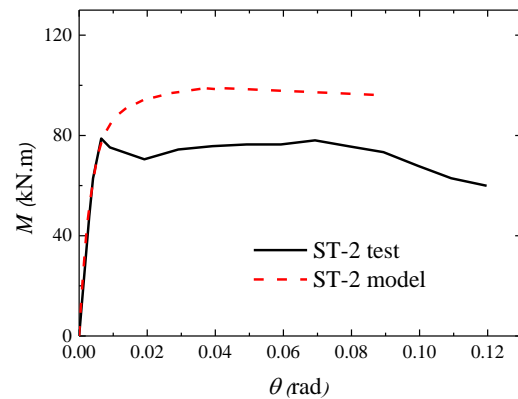
4. Finite Element Analysis and Test Result Comparison

The FE models were established and solved using the ABAQUS software. The moment-rotation curves attained by the numerical calculations are in comparison with the moment-rotation envelope curves obtained from the tests, as shown in Figure 8. The curves of specimens ST-1, ST-2, and ST-5 basically coincide in the early stage and demonstrate a few errors in the latter stage. The curves of the three other specimens basically coincide. The deviation between the curves is mainly caused by the following factors: (a) specimens ST-1, ST-2, and ST-5 suffer from severe concrete damage in the post-peak stage of test; (b) uncontrollable objective factors and human errors occurred during the test and cannot be considered in the FE model.

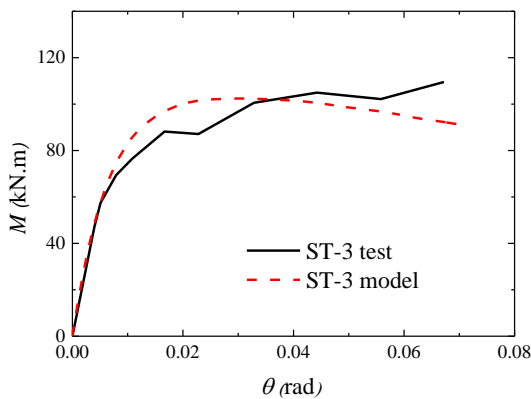
As shown in Figure 9, the comparison between failure modes of FEA and test shows that endplates in the finite element and in the test have undergone similar deformation, whether involving the thick endplate or the thin endplate. The weak beam connection in the test and FE model buckled at the root of the beam. The test and FE model basically have the similar failure modes. Therefore, the FE model is consistent with the tests and can be used for parameter analysis.



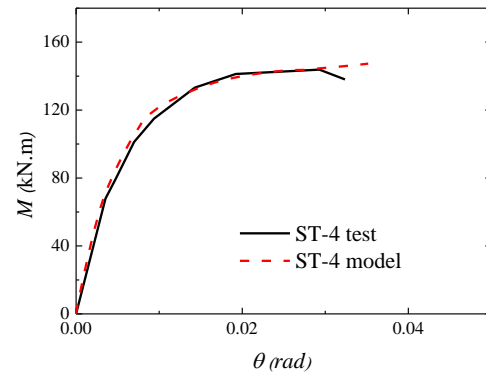
(a) ST-1



(b) ST-2



(c) ST-3



(d) ST-4

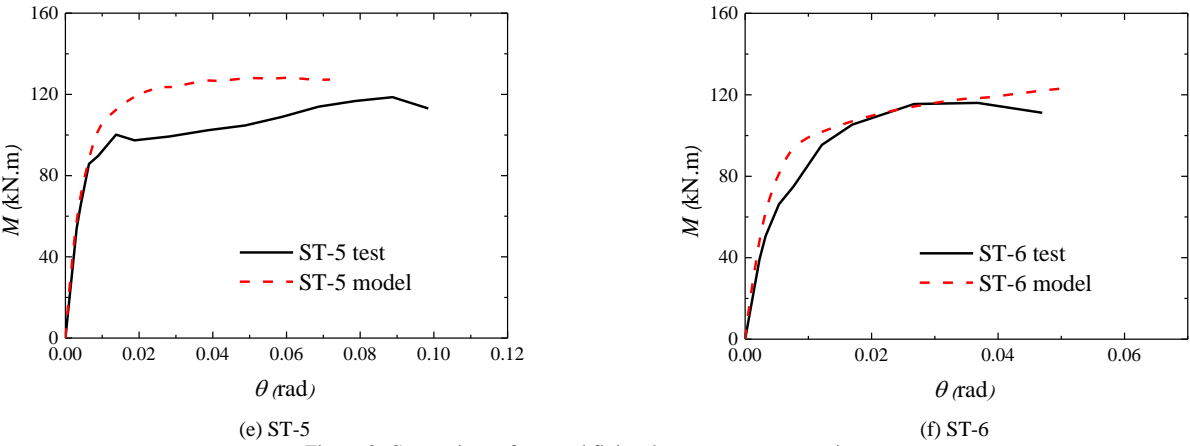


Figure 8. Comparison of test and finite element moment-rotation curves

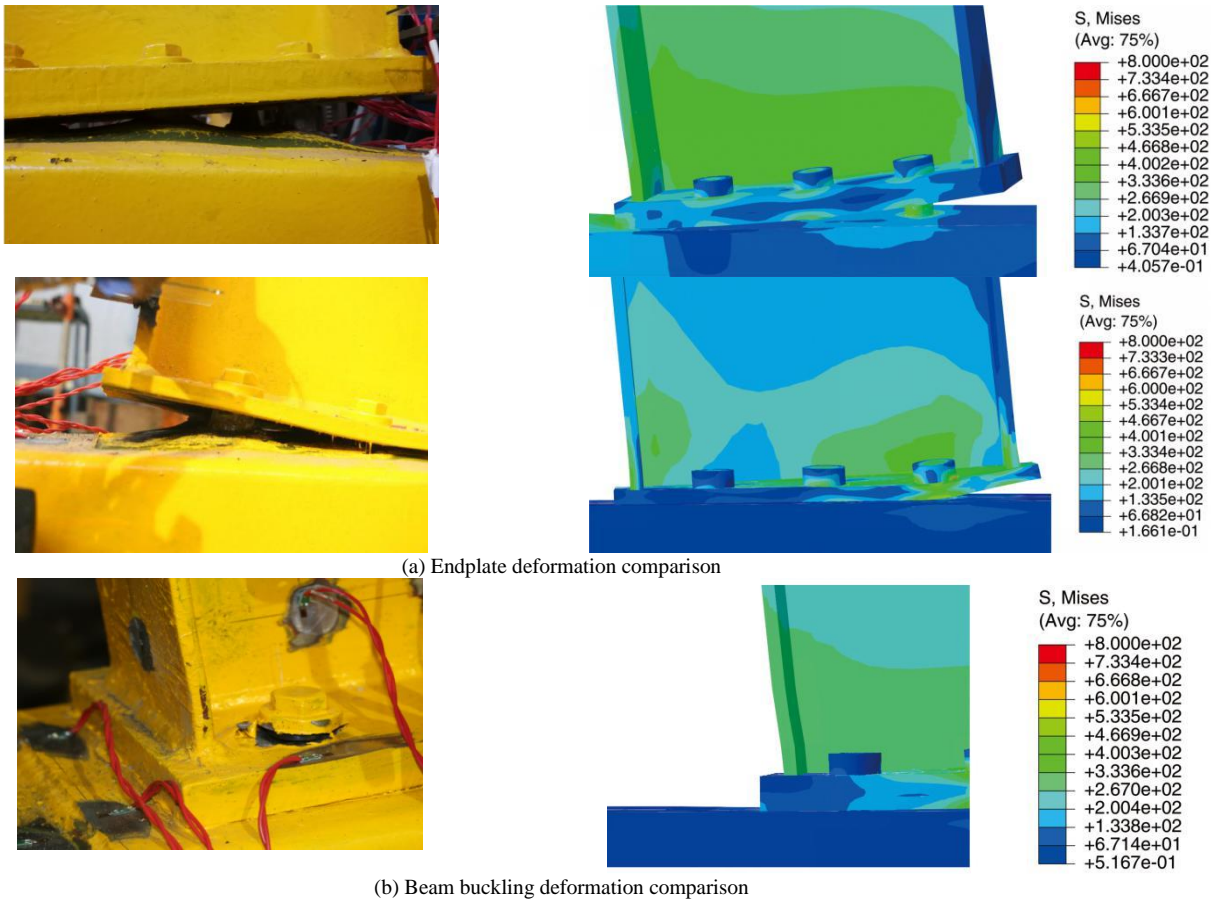


Figure 9. Comparison of the test and finite element failure modes

5. Analysis on Loading Transmission Mode

In the traditional CFT column connections, the load in the tensile area is mainly transmitted to the endplate through tensile flange of the h-shaped beam; thus, the endplate is bent. Subsequently, the load is transmitted to tubular wall of steel column through the bolts, leading to its apparent outward deformation of the tube.

However, the ABB connections to CFT columns, which are equipped with anchored bolts outrigger into the core concrete, effectively limit the outside deformation of the tubular walls. Thus, the load transmission mode and stress distribution of the anchored blind-bolted connections to CFT columns are different than those of the traditional CFT column

connections. On the basis of the verified FEA results of specimen ST-4, the internal stress distribution of the CFT column corresponding to the maximum moment is shown in Figure 10. The tensile force can be effectively transmitted to the entire threaded rod up to the anchored nut, indicating that the anchoring device can completely perform its function. The threaded rod transmits the tensile force to the concrete through the anchorage. The force transmission area is generally the cone with the anchor end as the vertex. The tensile force is then transmitted to the upper steel tubular wall. According to the FEA results, the diffusion angle of the cone is approximately 60° . Therefore, the area of the stress transmitted to the steel tubular wall is much higher than that of the connections without anchored bolts, in that the steel tubular wall is more uniformly stressed to achieve a smaller deformation. In addition, the stress is obviously concentrated at the anchored nut and around the sleeves. This result is consistent with the concrete deformation in the test. In conclusion, the transmission path of the load in the tensile area is given as follows: Steel beam--endplate--bolt--anchoring concrete--column wall. Clear description of the load transmission mode and stress distribution of the anchored blind-bolted connections to CFT column can facilitate the derivation of the calculation models and formulation for the rigidity and moment bearing capacity of such connections.

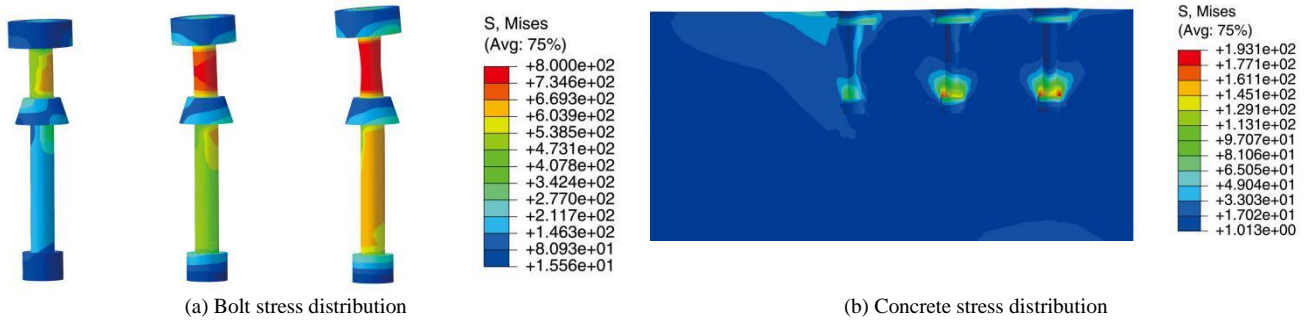


Figure 10. Stress distributions of the CFST columns

6. Parameter Analysis

The influences of strength grade of bolts, thickness of endplates, vertical interval between bolts, diameter of bolts, and pretension on bolts on the characteristics of the ABB connections to CFT columns were analyzed using the verified FE model. The basic calculating model included local reinforced CFT column, steel beam (HN350 \times 175 \times 7 \times 11 mm), and modified Hollo-Bolt.

6.1. Influence of Strength Grade of Bolts

The influence of strength grade of bolts on the moment-rotation curve of the connection is shown in Figure 11, which indicates that the strength grade of bolts does not influence the initial rotation stiffness of the connection. However, as the rotation of the connection increases, the connection with higher strength of bolts exhibits higher moment capacity. These results show that an increase in the bolt strength grade poses a certain influence on enhancing the rotation ability of the connection.

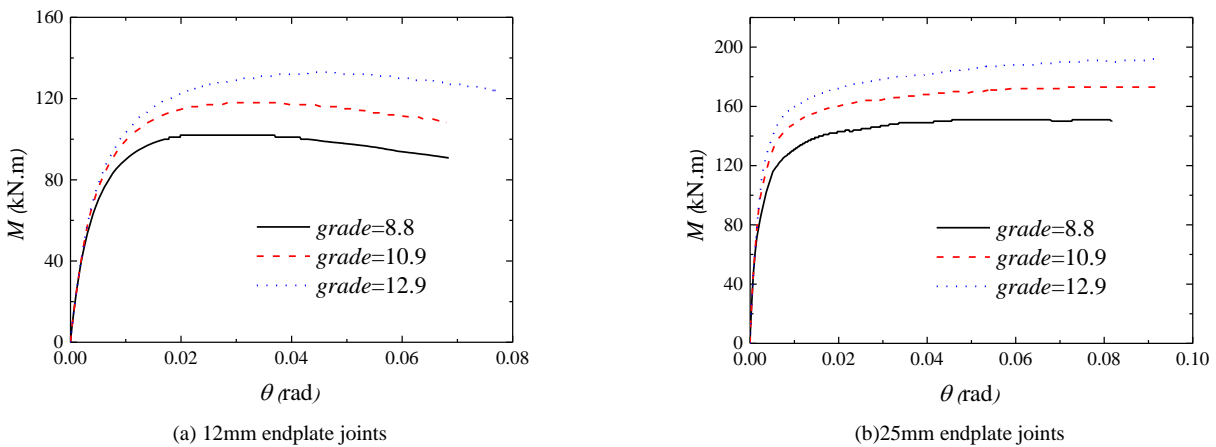


Figure 11. Influence of strength grade of bolts on connection performance

6.2. Influence of Thickness of Endplates

The influence of endplate thickness on the moment-rotation curve of the connection is shown in Figure 12, which indicates that the connection moment bearing capacity is increased with an increase in the thickness of endplates, but the yield rotation of the connection is decreased with an increase in the thickness of endplates, resulting in a low connection ductility. Furthermore, the initial stiffness of the connection increases with an increase in the endplate thickness. However, when the endplate reaches a certain thickness value, the influence on the initial stiffness of the connection is minimal with the increase in the endplate thickness.

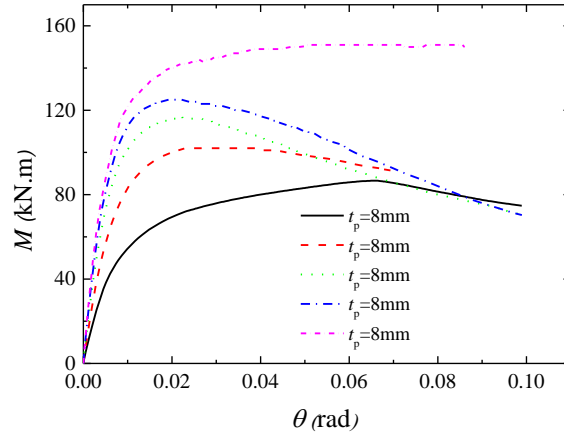
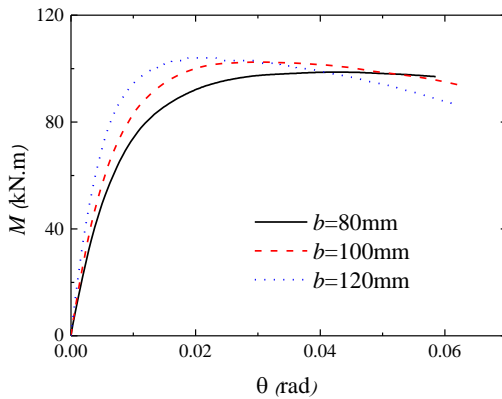


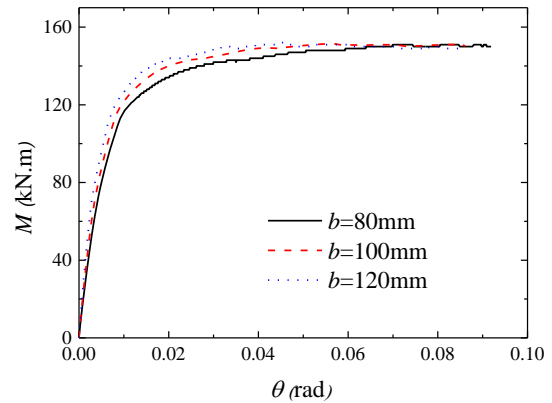
Figure 12. Influence of thickness of endplates on connection performance

6.3. Influence of Vertical Interval Between Bolts

The influence on the moment-rotation curves of the connection by vertical interval between bolts is shown in Figure 13, which indicates that the initial rigidity increases with an increase in the vertical interval between bolts, but the vertical interval has limited influence on the moment bearing capacity and yield moment of the connection. However, the curves show the corresponding connection rotation obviously increases with a decrease in the bolt interval. This result shows that a decrease in bolt interval can enable the bolt to reach the moment capacity at a larger rotation and increase the connection ductility. However, the connection stiffness can be low in the initial period. Therefore, the vertical connection spacing should be appropriate.



(a) 12mm endplate connections



(b) 25mm endplate connections

Figure 13. Influence of vertical interval between bolts on connection performance

6.4. Influence of Diameter of Bolts

The influence of diameter of bolts on the moment-rotation curves of the connection is shown in Figure 14, which indicates that an increase in the bolt diameter can increase the initial rigidity and moment bearing capacity of the connection. The

equivalent plastic strains of bolts in the FEA models are drawn. When the load displacement angle of the thick endplate specimens reaches 0.04 (load displacement angle upon the ST-4 connection at the failure in the test), the equivalent plastic strains of the M16–M20 bolts are 0.35, 0.31, and 0.22, respectively. These results show that the deformability increases with an increase in the bolt diameter. Hence, an increase in the bolt diameter is an efficient strategy to improve the bolt deformability.

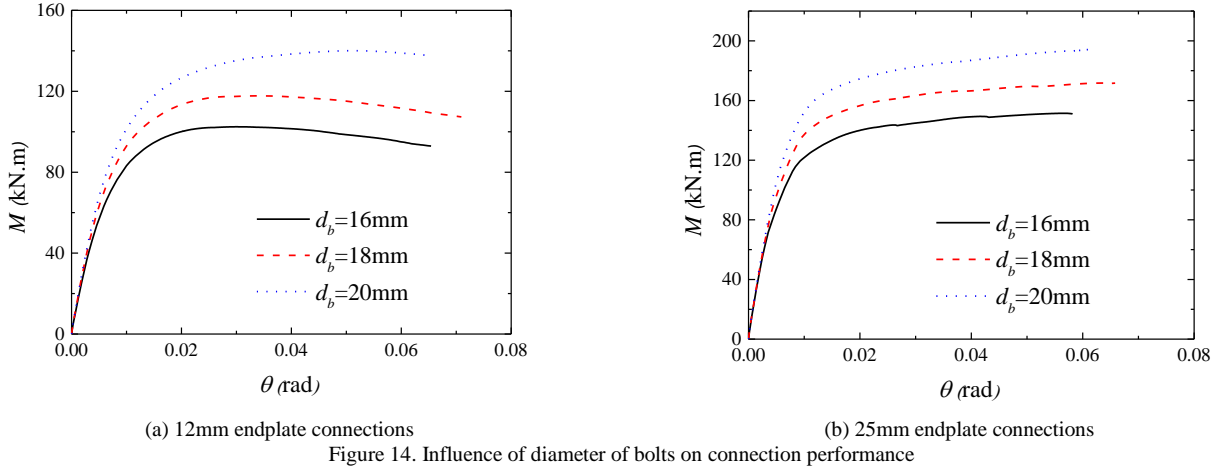


Figure 14. Influence of diameter of bolts on connection performance

6.5. Influence of Pretension on Bolts

The influence of pretension on bolts on the moment-rotation curve of the connection is shown in Figure 15. The pretension forces imposed on the grade 8.8 bolts and the grade 10.9 bolts are 70 and 100 kN respectively, in accordance with Chinese code GB50017-2003 [15]. The moment-rotation curves of both the grades 8.8 and 10.9 bolts basically coincide, indicating that different from common high-strength bolts, blind bolts aim to connect the hollow rectangular steel tubes and H-shaped beams by preloaded bolts before concrete is cast, and the anchoring role of concrete has a prominent influence on the connection performance when the load is applied on the connection. In this situation, the bolt pretension force has nearly no effect on the connection performance.

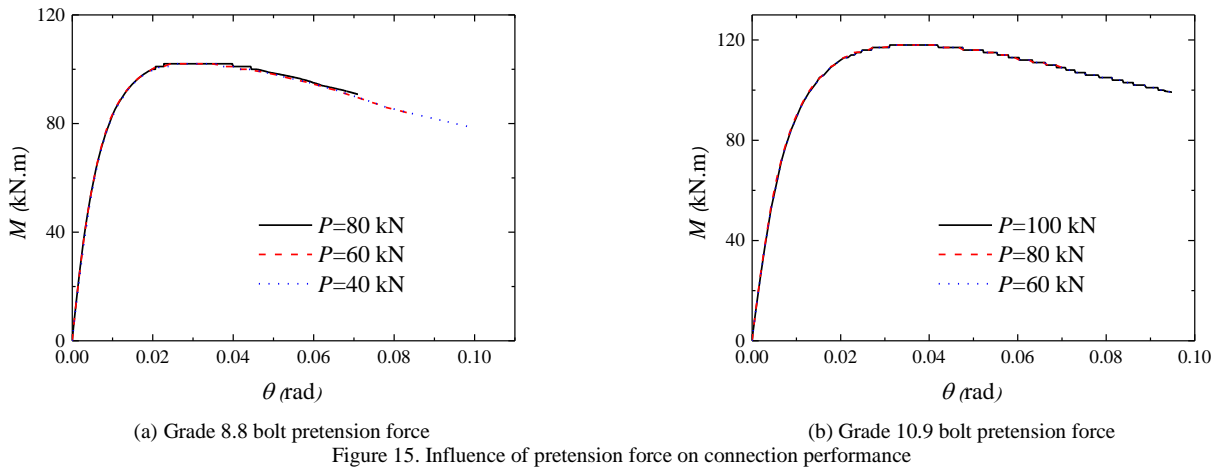


Figure 15. Influence of pretension force on connection performance

7. Stiffness Classification

According to EC3 Parts 1-8 [16], a connection can be classified as nominally pinned, semi-rigid, or rigid, depending on its rotational capacity. The detailed regulations are as follows:

Rigid connection: $K_i > k_b E_b I_b / L_b$;

Nominally pinned connection: $K_i < 0.5 k_b E_b I_b / L_b$;

Semi-rigid connection: $0.5 k_b E_b I_b / L_b < K_i < k_b E_b I_b / L_b$.

Where E is the elastic modulus of steel, I_b is the moment of inertia of the h-section steel beam, L_b is the beam span, and $k_b = 8$ is for the no-sway frame or $k_b = 8$ is for the sway frame. Therefore, all the six connections for test and 15 connections for FEA are semi-rigid ones. Therefore, the ABB flush endplate connections to CFT columns are typical semi-rigid connections.

8. Conclusions

The ABB connections to CFT columns were modeled and analyzed using the FEA software ABAQUS. The finite element and test results were compared and analyzed. The relevant parameters of the finite elements were also analyzed. The conclusions are drawn as follows:

(1) The FEA models were validated against the moment-rotation curves and the failure modes (the experimental observations) of the tested connections. The comparisons show that the FE model can excellently simulate the characteristics of the ABB connections to CFT columns.

(2) The tensile force can be effectively transmitted to the entire threaded rod up to the anchor nut, indicating that the anchoring device can completely perform its function. The threaded rod transmits the tensile force to the concrete through the anchorage. The force transmission area is generally the cone with the anchor end as the vertex. The tensile force is then transmitted to the upper steel tubular wall. According to the FEA results, the diffusion angle of the cone is approximately 60° .

(3) The initial rigidity and moment bearing capacity of the connection are influenced by endplate thickness and bolt diameter. The strength grade of bolts exerts an important influence on the moment bearing capacity, and the vertical interval between bolts mainly influences the initial stiffness. The bolt pretension force has minimal influence on the connection performance. According to the results of FEA, in engineering, the blind bolts can be strengthened by increasing the diameter of bolts, appropriately improving the strength grade of bolts and adopting an appropriate vertical interval between bolts in practical engineering.

(4) According to EC3 Parts 1–8, the ABB flush endplate connections to CFT columns are typical semi-rigid connections.

Acknowledgements

This work was financially supported through grants from the National Nature Science Foundation of China (No. 51638009, 51778241), State Key Laboratory of Subtropical Building Science, and South China University of Technology (No. 2017ZB28, 2017KD22). The authors thank the two anonymous reviewers for their helpful suggestions.

References

1. L. H. Han, W. Li, R. Bjorhovde, "Developments and Advanced Applications of Concrete-Filled Steel Tubular (CFST) Structures: Members," *Journal of Constructional Steel Research*, Vol. 100, pp. 211-228, 2014
2. S. Ellison and W. Tizanj, "Behaviour of Blind Bolted Connections to Concrete Filled Hollow Sections," *Structural Engineer*, Vol. 82, No. 22, pp. 16-17, 2004
3. A. Y. Elghazouli, C. Māaga-Chuquitaype, J. M. Castro, et al., "Experimental Monotonic and Cyclic Behaviour of Blind-Bolted Angle Connections," *Engineering Structures*, Vol. 31, No. 11, pp. 2540-2553, 2016
4. J. Wang, L. Zhang, B. F. S. Jr, "Seismic Response of Extended End Plate Joints to Concrete-Filled Steel Tubular Columns," *Engineering Structures*, Vol. 49, No. 2, pp. 876-892, 2013
5. J. F. Wang, L. H. Han, B. Uy, "Behaviour of Flush End Plate Joints to Concrete-Filled Steel Tubular Columns," *Journal of Constructional Steel Research*, Vol. 65, No. 4, pp. 925-939, 2009
6. J. Wang and L. Chen, "Experimental Investigation of Extended End Plate Joints to Concrete-Filled Steel Tubular Columns," *Journal of Constructional Steel Research*, Vol. 79, No. 12, pp. 56-70, 2012
7. W. Tizani and D. J. Ridley-Ellis, "The Performance of a New Blind-Bolt for Moment-Resisting Connections," Taylor & Francis, 2003
8. T. Pitrakos and W. Tizani, "Experimental Behaviour of a Novel Anchored Blind-Bolt in Tension," *Engineering Structures*, Vol. 49, No. 2, pp. 905-919, 2013
9. W. Tizani, A. Al-Mughairi, J. S. Owen, et al., "Rotational Stiffness of a Blind-Bolted Connection to Concrete-Filled Tubes using Modified Hollo-Bolt," *Journal of Constructional Steel Research*, Vol. 80, No. 1, pp. 317-331, 2013
10. W. Tizani, Z. Y. Wang, and I. Hajirasouliha, "Hysteretic Performance of a New Blind Bolted Connection to Concrete Filled Columns under Cyclic Loading: An Experimental Investigation," *Engineering Structures*, Vol. 46, No. 1, pp. 535-546, 2013
11. W. Tizani and T. Pitrakos, "Performance of T-Stub to CFT Joints using Blind Bolts with Headed Anchors," *Journal of Structural Engineering*, 2015

12. M. R. Bahaari and A. N. Sherbourne, "Behavior of Eight-Bolt Large Capacity End Plate Connections," *Computers & Structures*, Vol. 77, No. 3, pp. 315-325, 2000
13. L. H. Han, G. H. Yao, and X. L. Zhao, "Tests and Calculations for Hollow Structural Steel (HSS) Stub Columns Filled with Self-Consolidating Concrete (SCC)," *Journal of Constructional Steel Research*, Vol. 61, No. 9, pp. 1241-1269, 2005
14. SAC Joint Venture (SAC), Protocol for Fabrication, Inspection, Testing, and Documentation of Beam-column Connection Tests and Other Experimental Specimens, Rep. No. SAC/BD-97/02, SAC Joint Venture, Sacramento, California, USA, 1997
15. GB 50017-2003, Chinese Design Code of Steel Structure, Ministry of Housing and Urban-Rural Development of the People's Republic of China, Beijing, China, 2003
16. CEN, Eurocode 3: Design of steel structures-Part 1-8: Design of joints. ENV 1993-1-8, Brussels: CEN; 2005